

RAI Volume 3, Chapter 2.2.1.2.1, Sixth Set, Number 3:

Provide details of the parametric study that concluded appropriate variations in unconfined compressive strength for the five lithophysal rock categories would not affect significantly the results of the UDEC-Voronoi model. Describe how, for each rock-mass category, appropriate variations in unconfined compressive strength (e.g., SAR Figure 2.3.4-30) were used to calibrate and run the UDEC-Voronoi model.

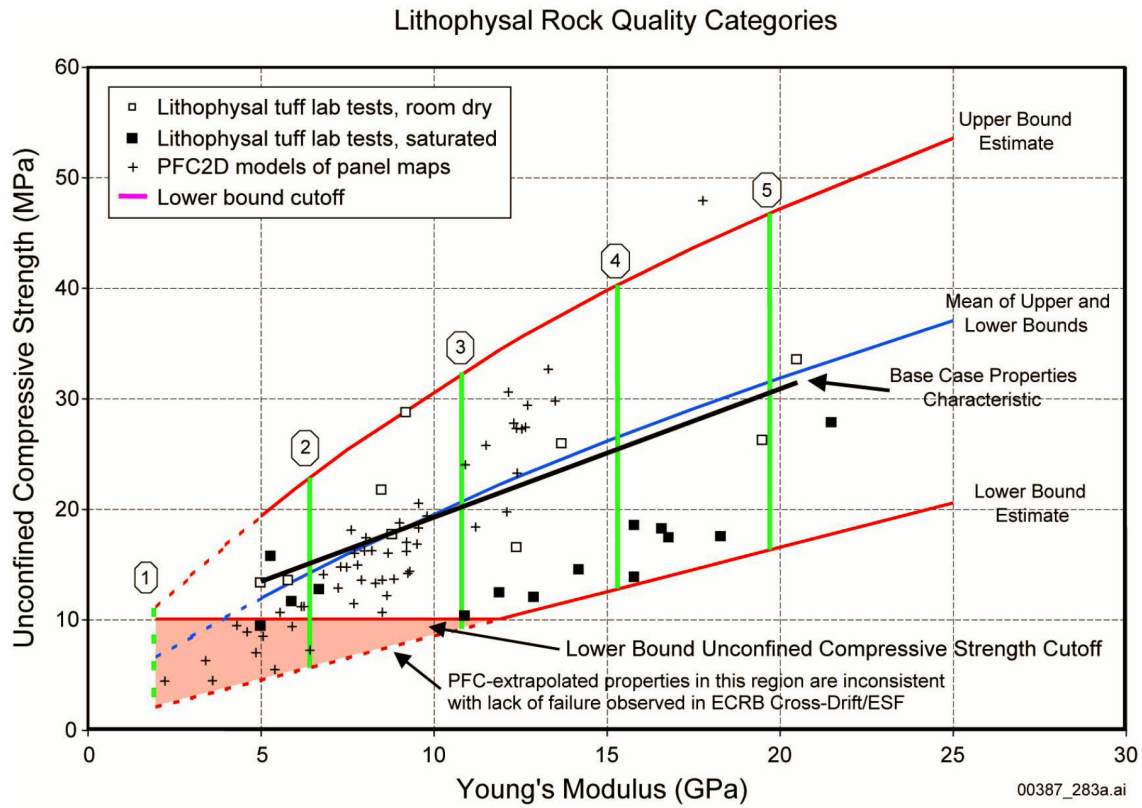
Basis: Spatial variability in rock properties can potentially affect models for drift collapse. DOE addressed this uncertainty by developing calibrated models for five different rock-strength categories, which are distinguished by different values of rock mass modulus. In conducting its calibration, DOE used the mean value of unconfined compressive strength as the calibration target for each selected value of rock mass modulus. DOE data show a large range of potential values of unconfined compressive strength for a given value of rock mass modulus (SAR, Figure 2.3.4-30). DOE stated (SAR, page 2.3.4-73) that a parametric study was conducted in which the Young's modulus and strength parameters were varied to account for the reasonable bounding ranges of lithophysal and nonlithophysal rock. DOE did not present results of analyses that showed appropriate ranges for rock strength were considered for the five lower lithophysal rock categories.

1. RESPONSE

This response provides the basis for and results from a parametric study demonstrating that the variability in unconfined compressive strength does not significantly affect the UDEC predictions of drift degradation in lithophysal units from thermal stress. Section 1.1 provides the basis for the lower bound in unconfined compressive strength that is used in the UDEC calculations for the parametric study. Section 1.2 presents the calibration of the UDEC model to the bounding values for unconfined compressive strength as a function of Young's modulus. Section 1.3 presents the results with the UDEC calibrated models for drift degradation during the first 10,000 years after closure.

1.1 LOWER BOUND FOR UNCONFINED COMPRESSIVE STRENGTH

The lithophysal rock mass has been categorized into five rock mass quality categories that span the range of strength and stiffness variations observed during mechanical testing of large-diameter cores taken from the lithophysal rock mass. The test results, base-case properties, and upper and lower bounds for the relationship between unconfined compressive strength (UCS) and Young's modulus are shown in Figure 1, which is identical to SAR Figure 2.3.4-30.



Source: SAR Figure 2.3.4-30.

Figure 1 Relation between UCS and Young’s Modulus for Lithophysal Rock Mass

The intersections of the vertical (green) lines with the black line in Figure 1 represent the base-case values of Young’s modulus and UCS used in the UDEC stability analyses of the emplacement drifts. Table 1 lists the base-case values of UCS and Young’s modulus for the five lithophysal rock strength categories. Table 1 also provides the porosity ranges for each rock category.

Table 1. Base-Case and Lower-Bound Strength Values for Rock Categories Used in UDEC Analyses of Spatial Variability

| Rock Category | Unconfined Compressive Strength (MPa) | | Estimated Young’s Modulus (GPa) | Approximated Lithophysal Porosity From Laboratory Tests (%) |
|---------------|---------------------------------------|-------------|---------------------------------|-------------------------------------------------------------|
| | Base Case | Lower Bound | | |
| 1 | 10 | 2.0 | 1.9 | 35 ± 8 |
| 2 | 15 | 5.6 | 6.4 | 28 ± 6 |
| 3 | 20 | 9.2 | 10.8 | 21 ± 4 |
| 4 | 25 | 12.8 | 15.3 | 13 ± 5 |
| 5 | 30 | 16.3 | 19.7 | 7 ± 7 |

Source: BSC 2004, Table E-11.

Figure 1 shows the scatter in the test results for UCS around the base-case line. Given this scatter, an estimated lower bound for UCS is defined by a solid red line in Figure 1, with numerical values provided in Table 1. Given the differences in base-case and lower-bound values for UCS in Table 1, a parametric study was performed to evaluate the potential impact of the variability in UCS on drift degradation in lithophysal rock units.

The parametric study is based on the lower-bound values for UCS in Table 1, with the additional constraint that the UCS should have a value of 10 MPa or greater. A minimum of 10 MPa is appropriate for UCS because lower values of UCS are inconsistent with the observed behavior in the Exploratory Studies Facility (ESF) and in the Enhanced Characterization of the Repository Block (ECRB) Cross-Drift. As discussed in *Drift Degradation Analysis* (BSC 2004, Sections E4.1.4.1 and E4.1.4.2), sections of the ESF and ECRB Cross-Drift would have shown significant damage and even rockfall from the drift walls under *in situ* conditions if the strength of the surrounding lithophysal rock mass were less than 10 MPa. However, the unsupported drift walls in the ESF and ECRB have remained in good condition, with no evidence of significant damage or rockfall. Based on these observations, the minimum value of UCS is defined as 10 MPa, and the lower-bound strength for rock mass categories 1, 2, and 3 is reset to 10 MPa. The lower bound for UCS, shown as a solid red line in Figure 1, includes the reset to 10 MPa.

Even with a cutoff or minimum of 10 MPa, the lower bound for UCS is conservative during the thermal period. The lower bound curve in Figure 1 is defined by test results for saturated cores, which are shown as solid black squares in the figure. The rock will dry out during the thermal pulse, so the UCS will be more similar to the test results for dry core, shown by the hollow black squares in Figure 1. As the test results for dry core are significantly greater than the test results for saturated core, the use of the lower bound for UCS does not accurately represent the strength of the lithophysal rock mass during the thermal pulse, particularly while the temperatures are greater than 100°C and thermally induced stresses are largest, because the rock will be dry. Regardless of this conservatism during the thermal dryout period, the parametric study is based on the lower-bound values for UCS (solid red line in Figure 1) to represent the greatest impact of the variability in UCS on drift degradation.

1.2 CALIBRATION OF THE VORONOI BLOCK MODEL TO LOWER-BOUND STRENGTH

The Voronoi block model was calibrated to the mechanical properties corresponding to the lower-bound strength envelope for rock mass categories 2, 3, 4, and 5. The calibration was carried out using the same procedure as discussed in *Drift Degradation Analysis* (BSC 2004, Section 7.6.4). Rock mass categories 2, 3, 4, and 5 constitute approximately 7 percent, 25 percent, 35 percent, and 30 percent, respectively, of the lithophysal rock mass (BSC 2004, Section 6.4.1.2 and Figure 6-115). Category 1 was not used for the parametric study because it represents only a few percent of the lithophysal rock mass; therefore, the amount of category 1 rock is so small that it cannot occur as a homogeneous rock mass on the scale of the drifts. Evaluation of the stability of a drift in a homogenous category 1 rock mass is, therefore, unrealistic, and this case was not performed during the parametric study.

The goal of the calibration is to match the values for Young's modulus and lower bound UCS listed in Table 1, with the exception that the value of UCS for categories 2 and 3 is reset to 10 MPa. The Voronoi block size for all calculations in the parametric study is 0.3 m (BSC 2004, Section 6.4.1.1).

Figure 2 shows the mode of failure of an unconfined core of lithophysal rock mass category 2 during calibration of the Voronoi model. It indicates the typical failure mode, which is mostly governed by axial splitting of the simulated core. The calculated stress-strain curve from this numerical experiment is shown in Figure 3. Two curves are shown: one calculated from the reaction forces at the bottom of the sample (green line), and the other calculated by averaging stresses in the middle of the sample (blue line). The curves are not identical, but they are sufficiently close to indicate that the model is nearly in equilibrium throughout the simulation. The curves indicate a UCS of approximately 10 MPa and Young's modulus (i.e., the slope of the loading portion of the curve) of 6.4 GPa, close to the target value in Table 1. The post peak response, with a sharp drop in the stress-strain curve after failure, is consistent with the relation between volumetric and axial strains (Figure 4); that is, the sample suddenly dilates after failure.

The effect of confinement for lower bound category 2, as determined by a separate numerical experiment, is illustrated by the stress-strain curve shown in Figure 5. Confinement of 1 MPa increases the compressive strength to approximately 14 MPa, and eliminates the sharp drop in the stress-strain curve after failure.

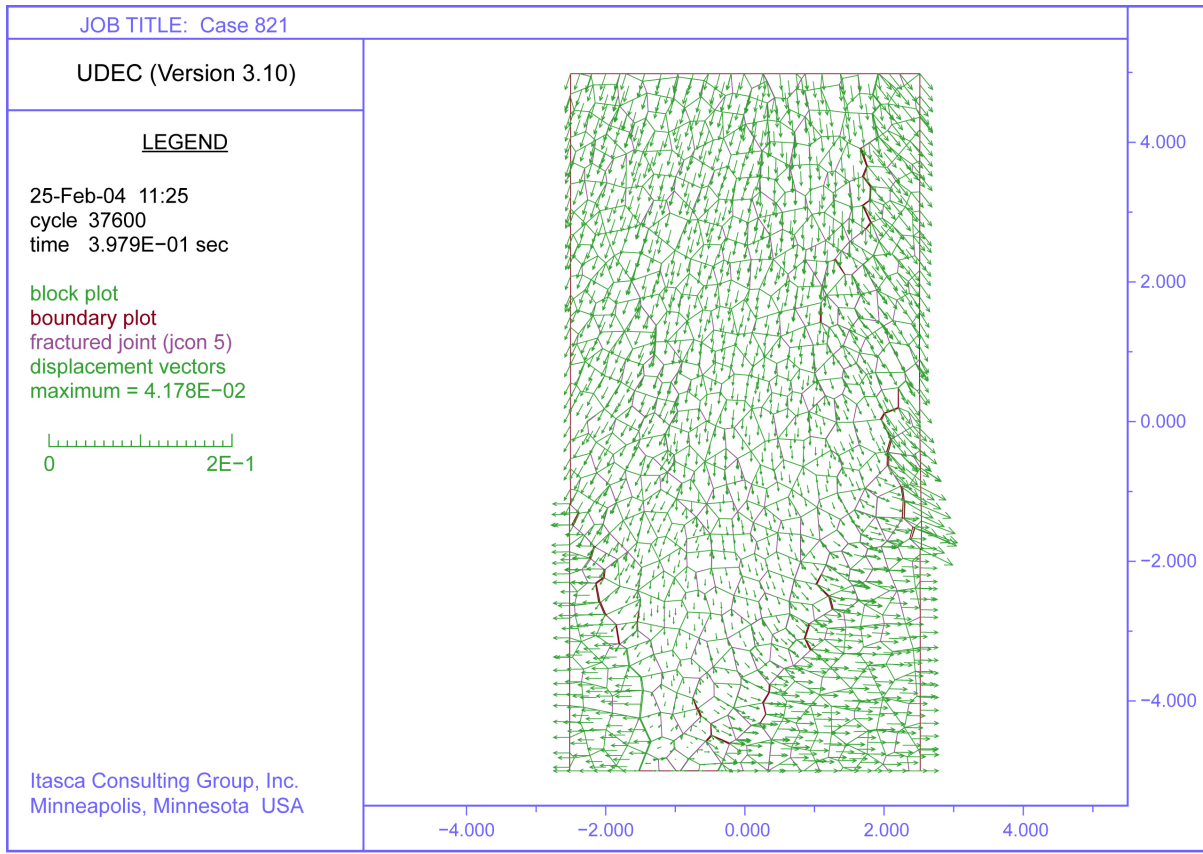
The stress-strain curves obtained during calibration for rock mass categories 3, 4, and 5 are shown in Figures 6 to 8. The additional plots for category 2 are not repeated for categories 3, 4, and 5 because they show qualitatively the same response. Figures 6 to 8 and Table 2 (based on the reactions at the bottom of the sample) illustrate that the target values of strength and stiffness, listed in Table 1, are well approximated by the calibrated Voronoi model. Figures 6 to 8 also illustrate the brittle response of the Voronoi block model under unconfined conditions, with a sharp drop in the stress-strain curve after failure.

Table 2. Mechanical Properties of the UDEC Voronoi Block Sample Calibrated to Lower-Bound Strength Envelope

| Rock Mass Category | Unconfined Compressive Strength* (MPa) | Young's Modulus** (GPa) |
|--------------------|----------------------------------------|-------------------------|
| 2 | 9.72 | 6.4 |
| 3 | 9.78 | 10.3 |
| 4 | 12.9 | 15.3 |
| 5 | 16.4 | 20.0 |

NOTES: *All data in the tables calculated based on the curves for the reactions at the bottom of the sample shown in Figures 3, 6, 7, and 8.

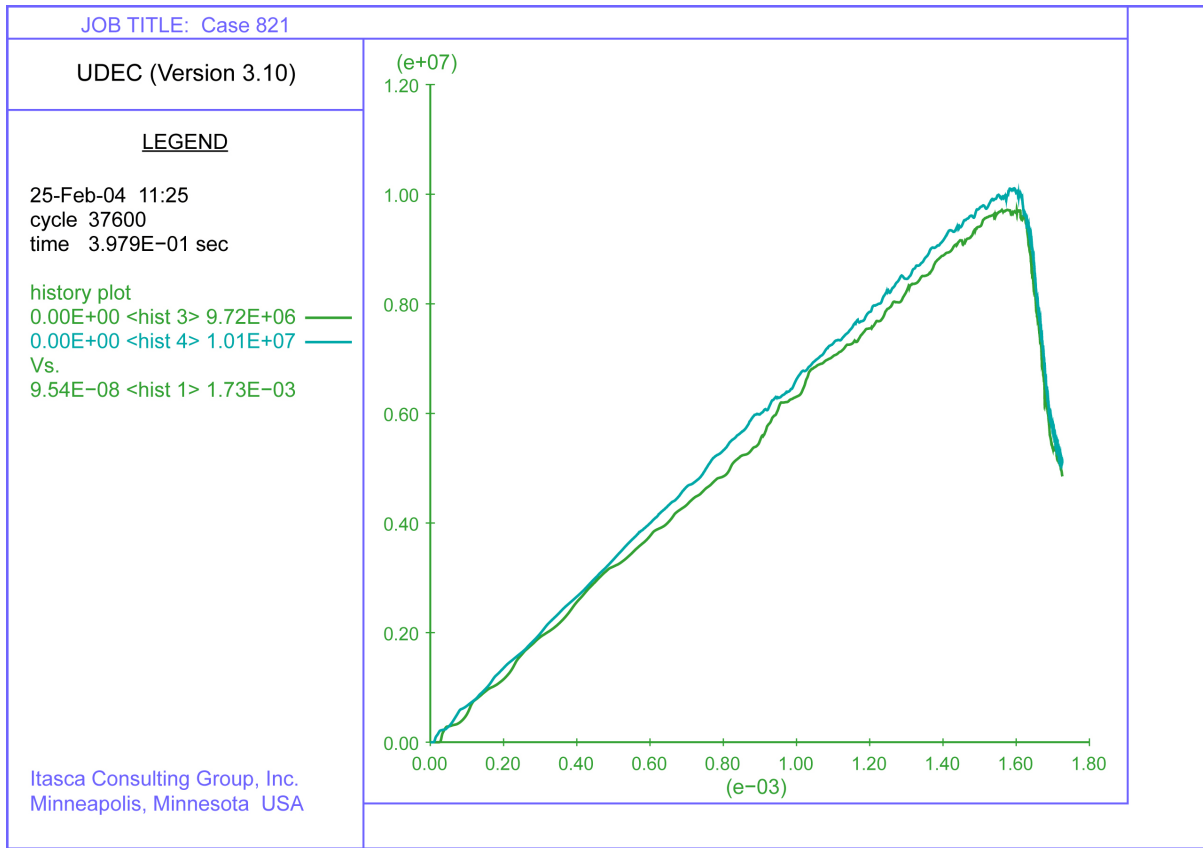
** Young's Moduli calculated as a slope of the line using the origin and a point roughly corresponding to 50% of the UCS.



02751DC_572.ai

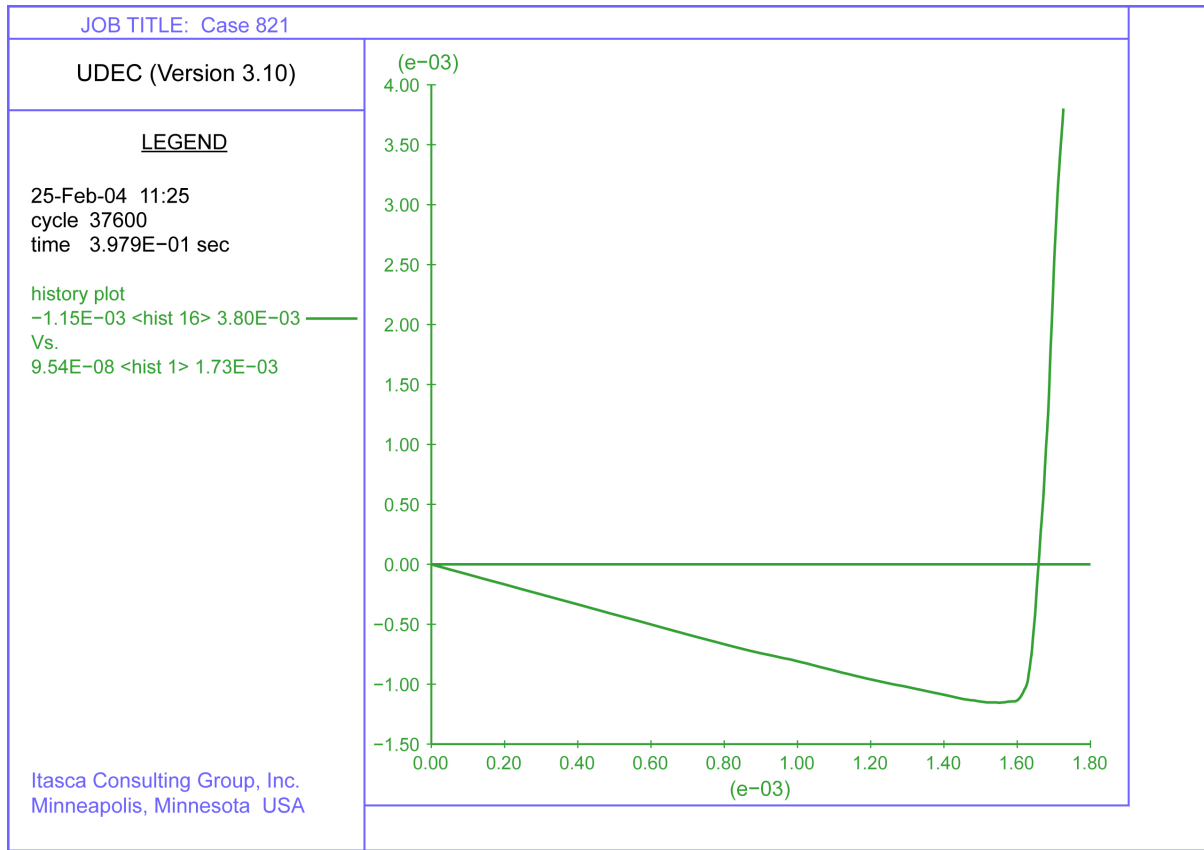
NOTE: Calculation for Category 2 lithophysal rock with a lower bound for unconfined compressive strength of 10 MPa . Distances and displacements are in meters.

Figure 2 Mode of Failure During Calibration of the Synthetic Sample of the Lithophysal Rock Mass under Uniaxial Loading Conditions



NOTE: The blue line (upper curve) is the stress calculated from the average stresses in the middle of the sample; the green line (lower curve) is the stress calculated from the reactions at the bottom of the sample.

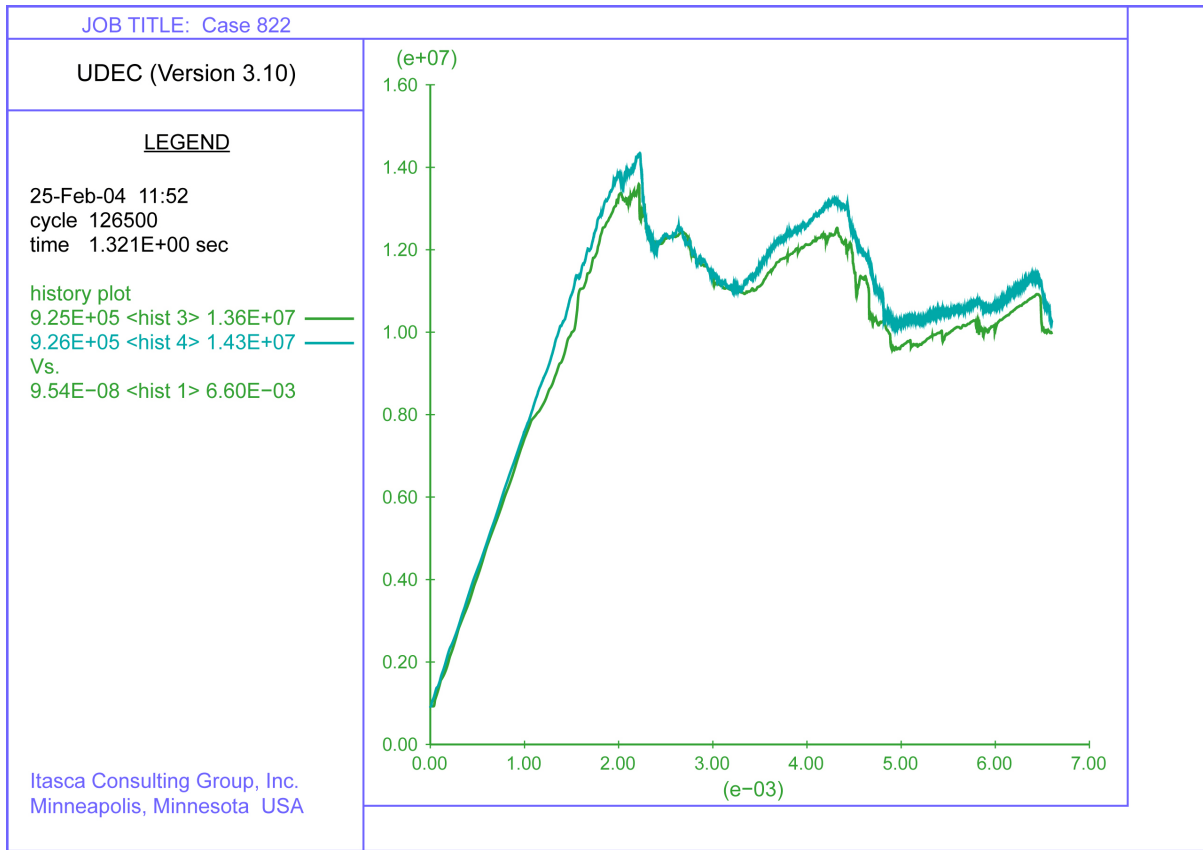
Figure 3 Stress (Pa) versus Strain (nondimensional) Curve for Unconfined Conditions for the Calibrated Properties of Category 2 Lithophysal Rock Mass for Lower-Bound Strength



02751DC_574.ai

NOTE: The horizontal line intersecting 0.00 on the y-axis is a plot axis, and does not represent volumetric strain.

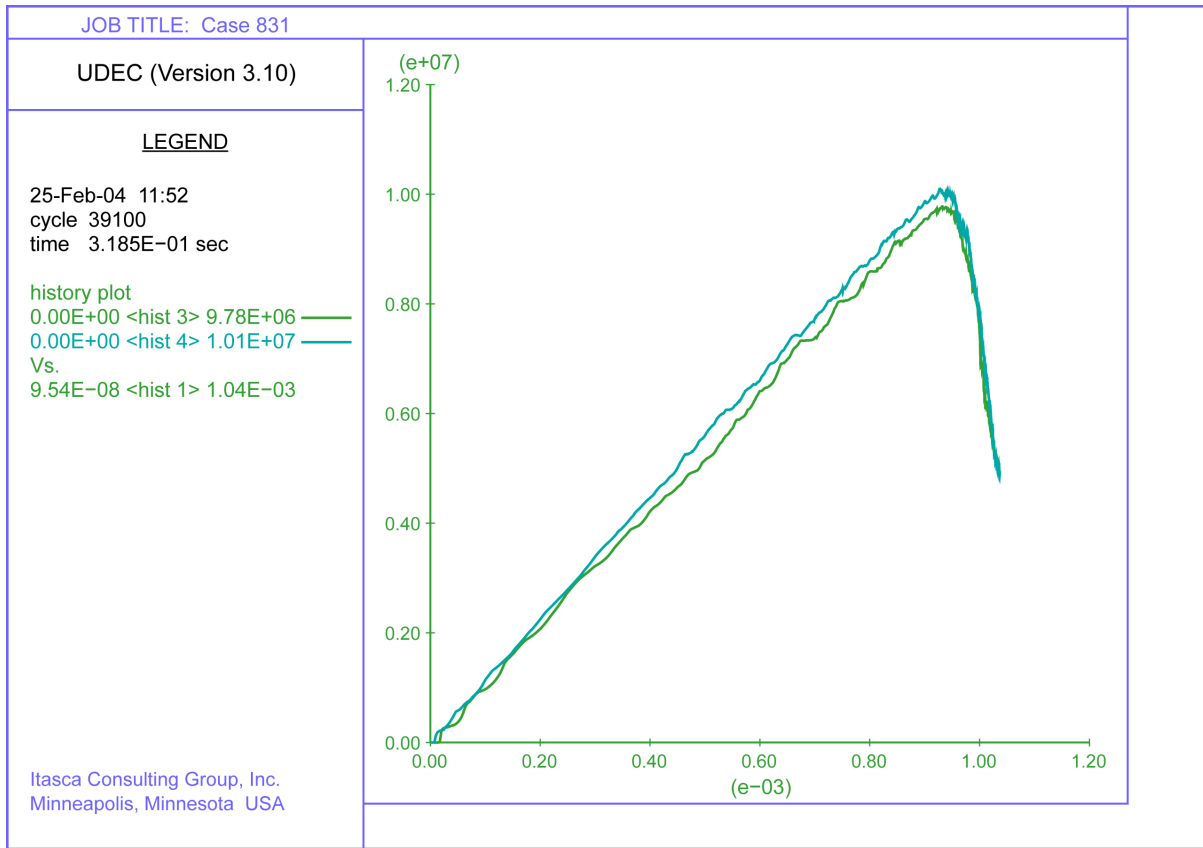
Figure 4 Volumetric strain (nondimensional) versus Axial Strain (nondimensional) Curve for Unconfined Conditions for the Calibrated Properties of Category 2 Lithophysal Rock Mass for Lower-Bound Strength



02751DC_575.ai

NOTE: The blue line (upper curve) is the stress calculated from the average stresses in the middle of the sample; the green line (lower curve) is the stress calculated from the reactions at the bottom of the sample.

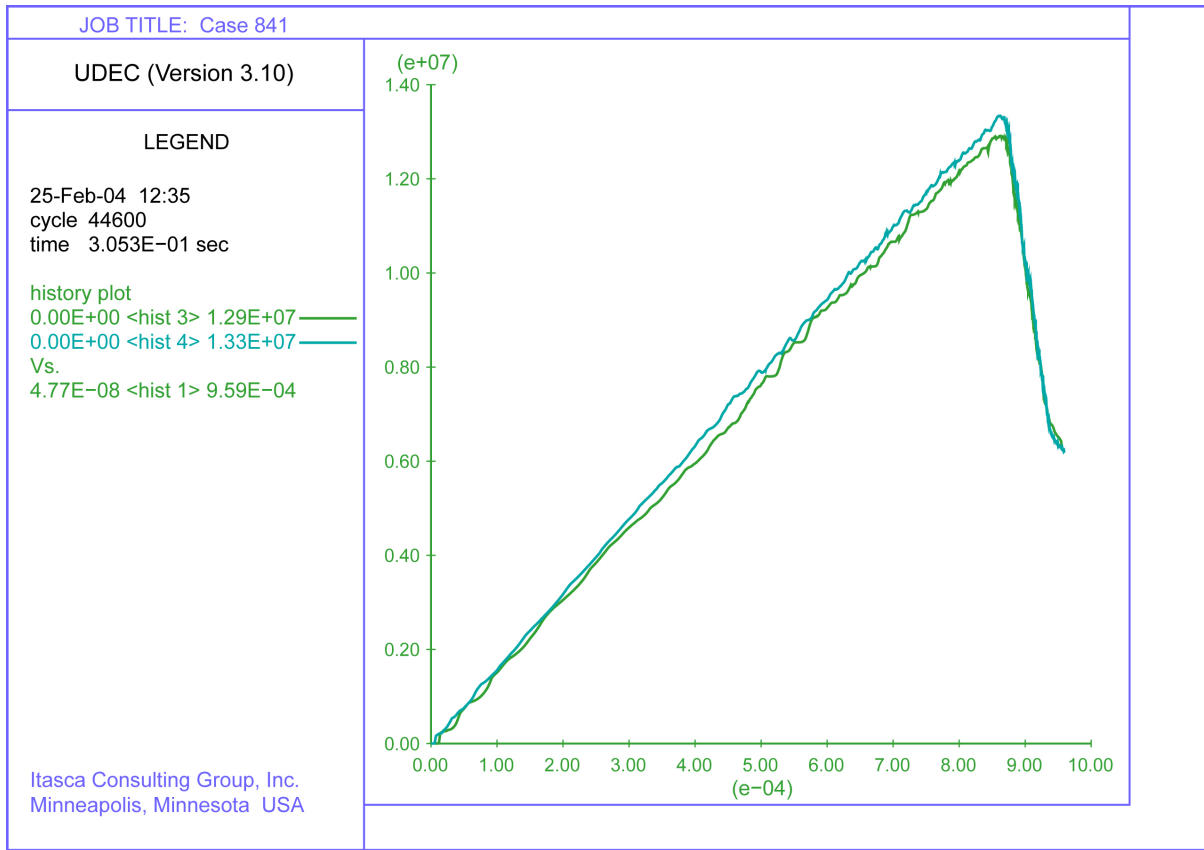
Figure 5 Stress (Pa) versus Strain (nondimensional) Curve for 1-MPa Confinement for the Calibrated Properties of Category 2 Lithophysal Rock Mass for Lower-Bound Strength



02751DC_576.ai

NOTE: The blue line (upper curve) is the stress calculated from the average stresses in the middle of the sample; the green line (lower curve) is the stress calculated from the reactions at the bottom of the sample.

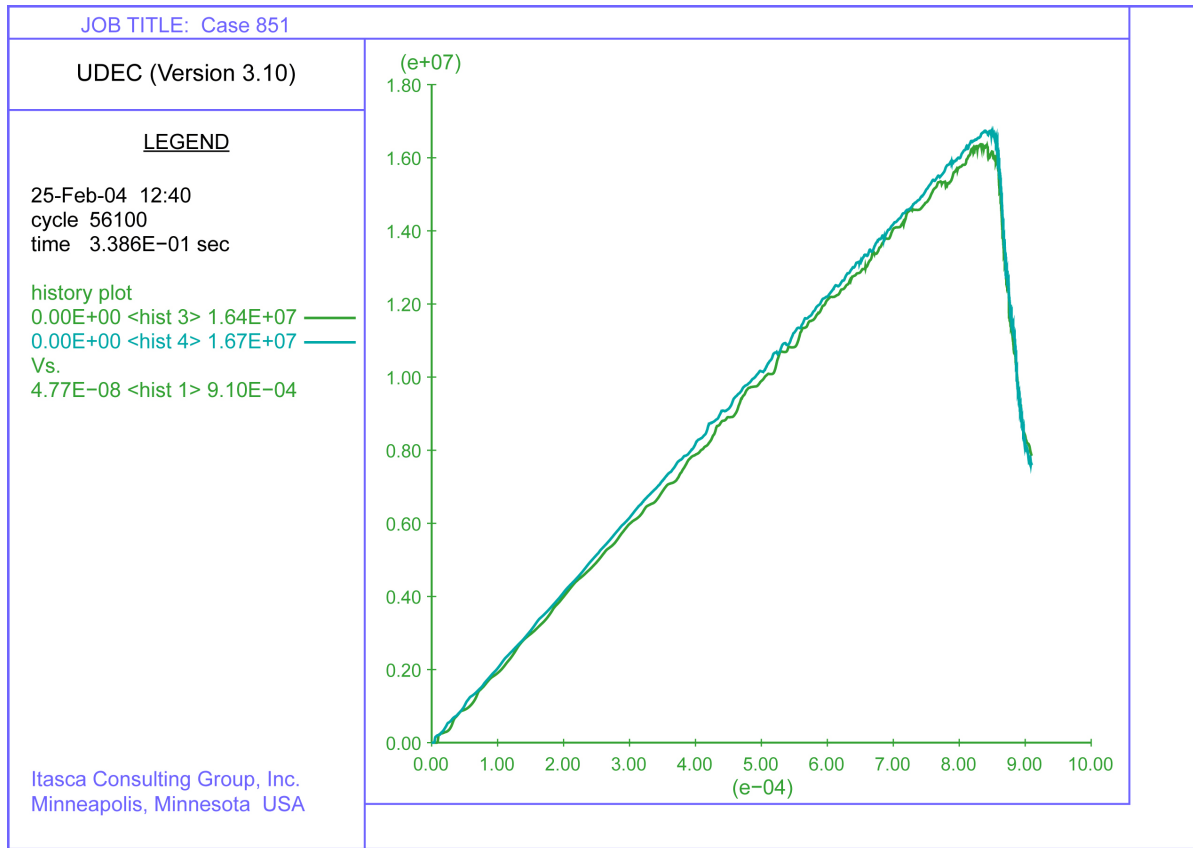
Figure 6 Stress (Pa) versus Strain (nondimensional) Curve for Unconfined Conditions for the Calibrated Properties of Category 3 Lithophysal Rock Mass for Lower-Bound Strength



02751DC_577.ai

NOTE: The blue line (upper curve) is the stress calculated from the average stresses in the middle of the sample; the green line (lower curve) is the stress calculated from the reactions at the bottom of the sample.

Figure 7 Stress (Pa) versus Strain (nondimensional) Curve for Unconfined Conditions for the Calibrated Properties of Category 4 Lithophysal Rock Mass for Lower-Bound Strength



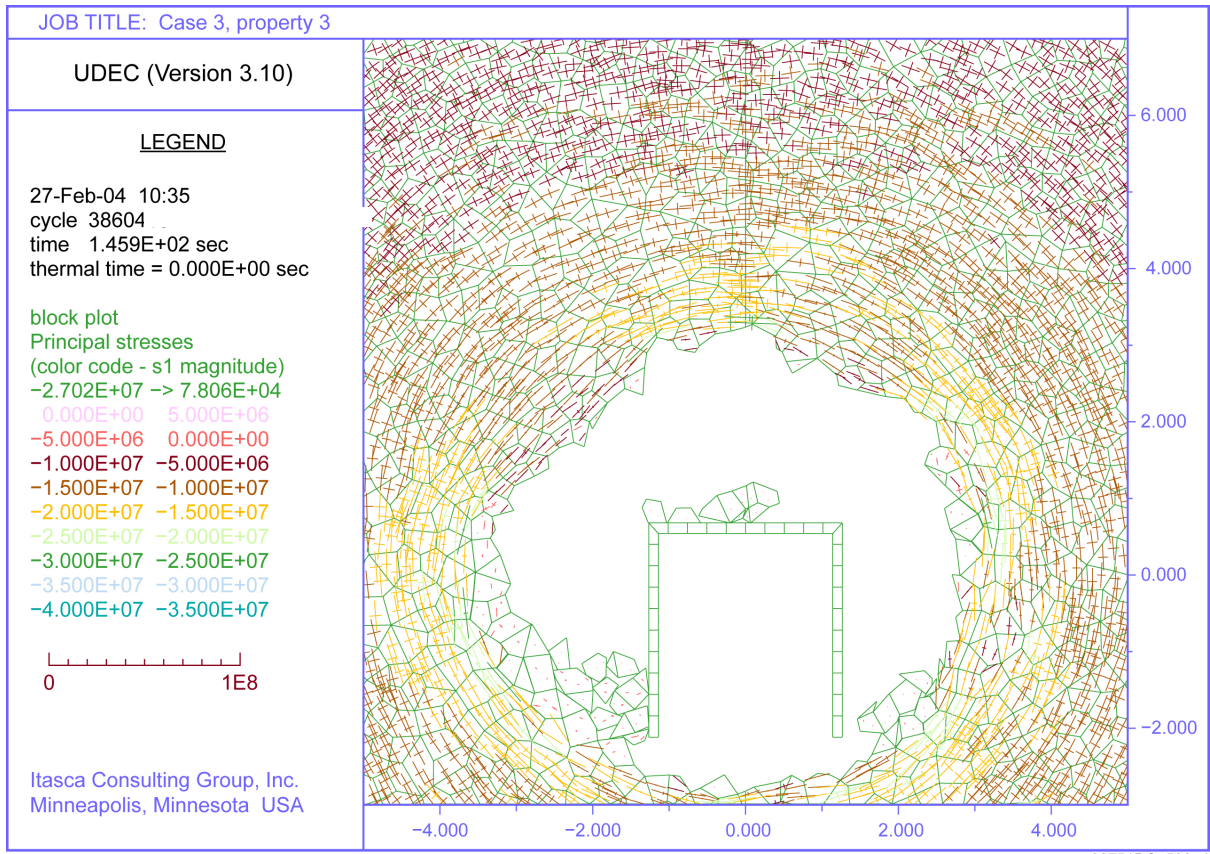
02751DC_578.ai

NOTE: The blue line (upper curve) is the stress calculated from the average stresses in the middle of the sample; the green line (lower curve) is the stress calculated from the reactions at the bottom of the sample.

Figure 8 Stress (Pa) versus Strain (nondimensional) Curve for Unconfined Conditions for the Calibrated Properties of Category 5 Lithophysal Rock Mass for Lower-Bound Strength

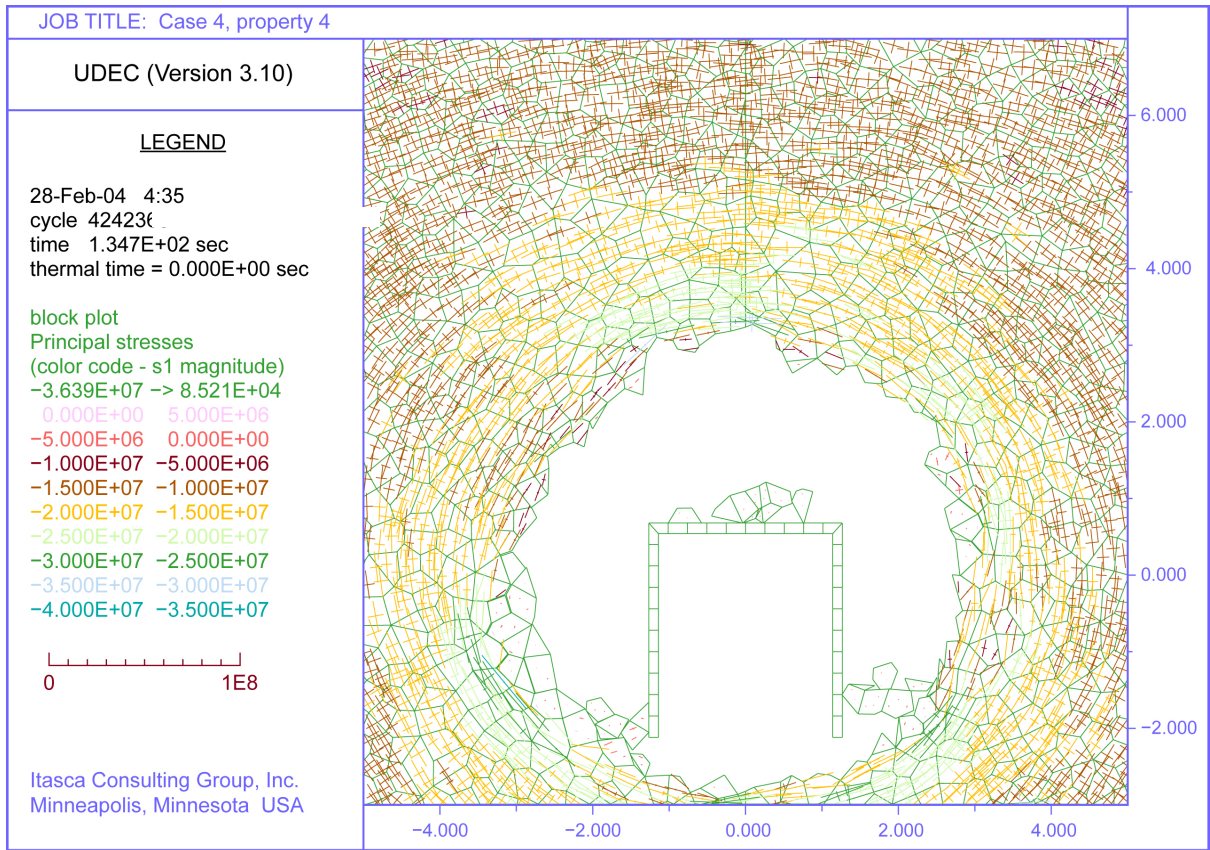
1.3 DRIFT STABILITY FOR LOWER-BOUND STRENGTH ENVELOPE FOR THERMAL LOADING CONDITIONS

A drift stability analysis was performed with the calibrated Voronoi block models for the lower-bound strength envelope for lithophysal rock mass categories 2, 3, 4, and 5 using the methodology described in detail in *Drift Degradation Analysis* (BSC 2004, Section 6.4.2.3). The initial drift configuration is 5.5 meters in diameter and the drip shield is approximated as a rigid, rectangular structure that rests on the bottom of the drift (BSC 2004, Figure 6-116 and Section 6.4.2.1). The invert, pallet, and waste package are not represented in this model (BSC 2004, Section P2.1). The results are summarized in Figures 9 to 12, which show the drift configurations and associated stress tensors colored by the magnitude of the major principal stress at 80 years after waste emplacement, equivalent to 30 years after closure, when maximum thermal stresses are reached. It is important to note that the analyses were carried out until 10,000 years after closure, but no additional rockfall took place after 80 years for any of the 4 rock mass categories.



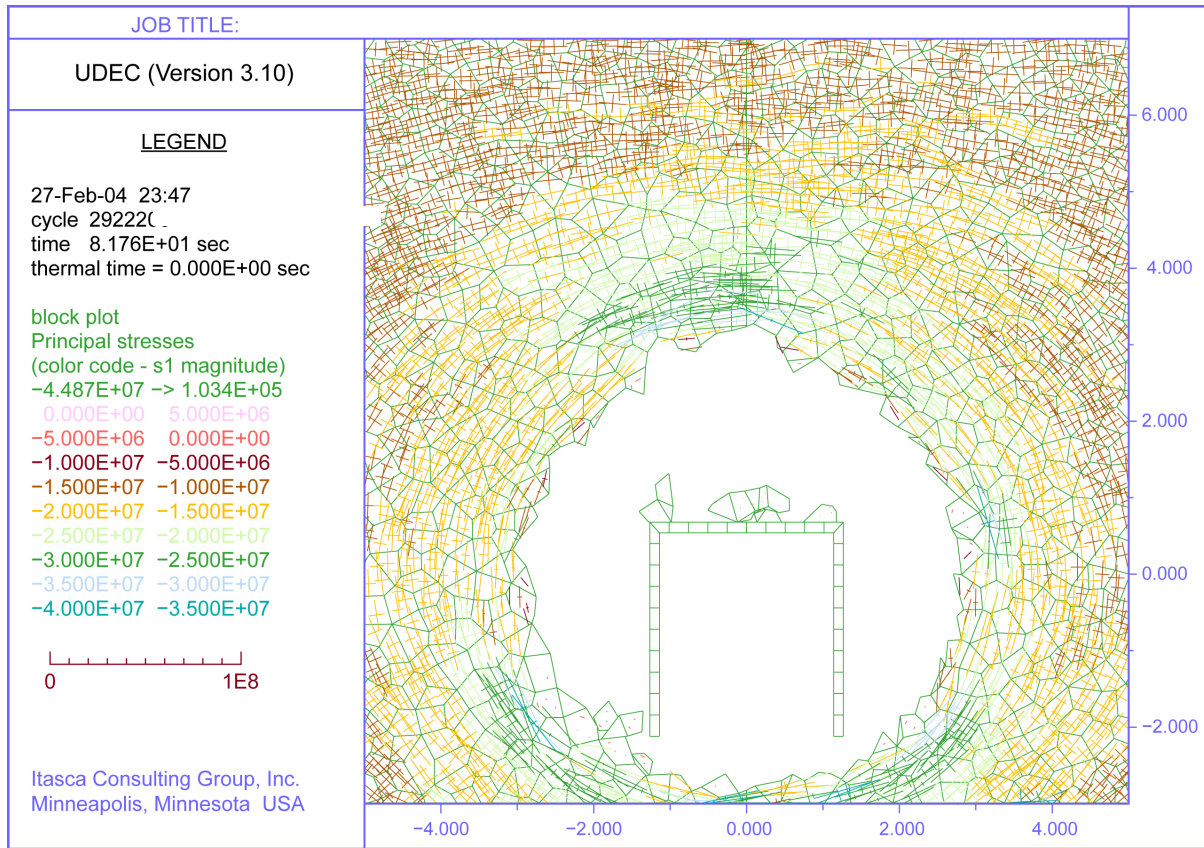
NOTE: The color scale is based on the magnitude of the major principal stress. Distances are in meters.

Figure 10 Stresses (Pa) and Drift Configuration 80 Years After Emplacement of Waste in Lithophysical Rock Category 3 with Lower Bound UCS



NOTE: The color scale is based on the magnitude of the major principal stress. Distances are in meters.

Figure 11 Stresses (Pa) and Drift Configuration 80 Years After Emplacement of Waste in Lithophysal Rock Category 4 with Lower Bound UCS



02751DC_582.ai

NOTE: The color scale is based on the magnitude of the major principal stress. Distances are in meters.

Figure 12 Stresses (Pa) and Drift Configuration 80 Years After Emplacement of Waste in Lithophysal Rock Category 5 with Lower Bound UCS

1.4 CONCLUSIONS

The analysis for the base-case (mean) properties documented in *Drift Degradation Analysis* (BSC 2004, Section 6.4.2.3.1) indicates virtually no rockfall due to thermal loading for any rock mass category. If the properties corresponding to the lower-bound strength envelope are assumed, the predicted rockfall for rock mass categories 2 to 5 remains relatively small, as shown in Figures 9 to 12. Breakout occurs from the crown of the drift, up to a depth of 0.5 meters, for all rock mass categories. Destressing and unraveling is also observed from the drift walls for rock mass categories 2 and 3, with UCS of 10 MPa. These results demonstrate minor rockfall from thermal stresses with the lower bound UCS, confirming that the variability in unconfined compressive strength, as shown in SAR Figure 2.3.4-30, does not significantly affect the UDEC predictions of drift degradation in lithophysal units from thermal stress.

2. COMMITMENTS TO NRC

None.

3. DESCRIPTION OF PROPOSED LA CHANGE

None.

4. REFERENCES

BSC (Bechtel SAIC Company) 2004. *Drift Degradation Analysis*. ANL-EBS-MD-000027 REV 03. Las Vegas, Nevada: Bechtel SAIC Company. ACC: DOC.20040915.0010; DOC.20050419.0001; DOC.20051130.0002; DOC.20060731.0005.